

POLYCRYSTALLINE MICROSTRUCTURE AND SCATTER IN THE NUMBER OF CYCLES TO INITIATION OF A HIGH-CYCLE FATIGUE CRACK

M. Sauzay, Th. Jourdan
DEN-DMN-SRMA, CEA, France

ABSTRACT

This paper is dedicated to an attempt to model the link between random microstructures and initiation characteristics of high-cycle fatigue of polycrystals (scatter, grain size effect). Crack initiation often takes place along slip bands. This mechanism is modeled using an energy criterion. Statistical computations permit us to take into account random microstructures. Predictions are compared to experimental results and are discussed with respect to the influence of crystalline cubic elasticity on scatter. A strong cubic elasticity anisotropy (austenite, copper) induces scatter in the resolved shear stress in the well-oriented grains because of neighbour effects. But it not high enough for inducing a significant scatter in the number of cycles to crack nucleation for usual specimen and grain sizes.

1 INTRODUCTION

Based on observations, the main part of the high-cycle fatigue lifetime corresponds to initiation and propagation of microstructurally short cracks (stage I) [1]. During stage I, the local microstructure (crystallographic orientations, grain sizes...) is of great importance. Initiation and propagation/arrest of a given short crack depend in fact on its local environment [2]. These observations explain partially the high scatter in the number of cycles to failure which is classically observed when carrying out high-cycle fatigue tests [3]. Even if two specimens are identical at the macroscopic scale, their local microstructures at the grain scale are different. Surface defects and experimental problems are other sources of scatter, but even if they are the smallest possible, a high degree of scatter is still observed. Concerning high-cycle fatigue properties, a grain size effect is usually observed too [4] and sometimes a specimen size effect [5]. All these observations could be characteristic of the initiation and/or short crack propagation periods. For the sake of simplicity, only short crack initiation is considered in the following. This is defined as the germination of a crack of one grain size length (before eventually propagating through other grains). This paper proposes a model of the link between random microstructures and initiation characteristics of high-cycle fatigue of polycrystals. Modeling is divided into two steps. First, the most common crack initiation mechanism in polycrystals is modeled using an energy criterion following the proposition of Mura and co-workers [6,7]. Second, thanks to statistical computations, random microstructures are taken into account. Predictions are compared to experimental results and discussed with reference to the influence of cubic elasticity.

2 MODELLING

1.1 Crack initiation in a given (well-oriented) grain.

Based on large number of observations on metal/alloy single crystals and polycrystals, crack initiation along (or inside) fatigue slip bands is the one of the main causes of damage initiation [8]. Plastic strain is localized in thin slip bands which appear in well-oriented grains (those with a high shear stress on

one of their slip systems). They are often associated to Persistent Slip Bands (PSBs). Cycle by cycle, accumulated plastic slip, stored energy and stress level increase due to plastic irreversibilities [8,6,7]. Finally, cracks appear along slip bands and then can propagate. In the 80s, Mura and co-workers proposed a crack initiation criterion based on an energy balance. Cracks appear only when the cycle by cycle stored energy is higher than the surface energy required for free surface creation. The variation of stored energy between the initial and the cracked solid would then be higher than the required surface energy. The initiated crack length is assumed to be of one grain size. This model gives the number of cycles required for crack initiation in a grain whose well-oriented slip system is submitted to a resolved shear stress τ :

$$N_{ini} = C \frac{\mu \gamma_s}{\Phi p^2 (1-\nu)^2} \frac{1}{(\tau - \tau_0)^3} \quad (1)$$

with C a material parameter, μ and ν the isotropic elastic parameters, γ_s the free surface energy, Φ the grain size, p the irreversibility factor and τ_0 the critical shear stress for slip band apparition [7].

1.2 Statistical computations.

In the following, only surface grains are considered because crack initiation occurs preferentially on the free surfaces of the specimen [7]. The specimen gauge characteristic size is denoted as D (length and diameter order of magnitude). There are about $k=(D/\Phi)^2$ surface grains along the gauge length (Fig. 1 a)). If a crack initiates in the i^{th} grain, it is assumed to appear along its most loaded slip plane submitted to a τ_i shear stress. All the grains are assumed to have the same grain size. The first crack appears in the grain whose maximal shear stress on its slip system is the highest of all the grains. Therefore, the number of cycles to initiation at the free surface of a specimen is:

$$N_{ini} = C \frac{\mu \gamma_s}{\Phi p^2 (1-\nu)^2} \frac{1}{\left(\max_i (\tau_i) - \tau_0 \right)^2} \quad (2)$$

The stress distribution of the shear stress in the k grains is now considered in order to compute the distribution of the number of cycles to initiation given by eqn (2). The cumulated probability of the resolved shear stress in a grain is denoted as $F_i(\tau)$. For example if both cubic elasticity anisotropy and plasticity are neglected, the stress tensor is homogeneous in the polycrystal and is equal to the macroscopic one. For a tensile test, the resolved shear stress in the i^{th} grain is given by: $|\tau_i|=f_i \Sigma$. The Schmid factor in the i^{th} grain is denoted as f_i . Then, the cumulated density is deduced from the Schmid factor cumulated density (Fig. 1 b)). It is given for a torsion test too. For a torsion loading, the tensile stress Σ should be replaced by $2T$ (T is the macroscopic shear stress). If cubic elasticity is rather anisotropic (copper, austenitic stainless steel) or (and) plasticity is (are) non-negligible, then more sophisticated shear stress distributions have to be computed (see discussion below). If the maximal resolved shear stress is smaller than τ , its value in each grain, τ_i , has indeed to be smaller than τ . As the stress field is homogeneous, the stress distribution in a given grain does not depend on the stress distributions in the other grains. This is why the product of the grain probabilities is obtained giving

eqn (3). Whatever is the shear stress distributions F_{τ} , the maximal resolved shear stress distribution at the surface of the specimen is indeed given by:

$$F_{\tau,k}(\tau) = (F_{\tau}(\tau))^k \quad (3)$$

For initiation before the N_{ini}^{th} cycle, the resolved shear stress in at least one grain has to be higher than $\tau(N_{ini})$ which is defined as the stress satisfying eqn (1) for a given N_{ini} value.

Finally, the cumulated probability of the number of cycles to crack initiation is deduced:

$$F_N(N_{ini}) = 1 - F_{\tau,k}(\tau(N_{ini})) \quad (4)$$

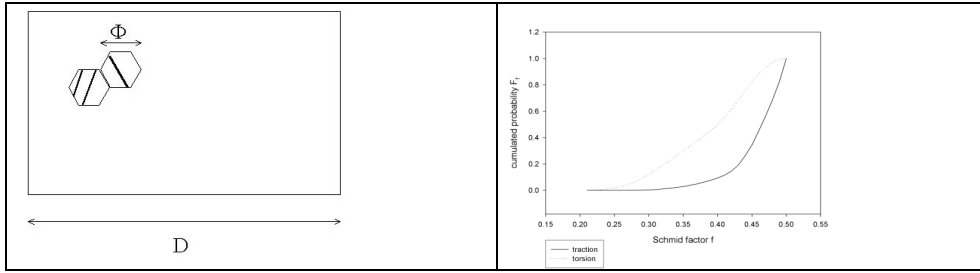


Figure 1: a) polycrystal surface view, slip bands are visible; b) Schmid factor distribution in a random Face Cubic Centred (FCC) polycrystal (computations on a large number of grains whose crystallographic orientations are random). Tension-compression and torsion loadings.

This distribution can be easily computed using eqns (1)-(4). It depends on the resolved shear stress distribution, material parameters, loading, specimen and grain sizes.

3 FIRST RESULTS

In this part, the resolved shear stress distribution using the Schmid factor distributions (Fig. 1 b), FCC polycrystal without macroscopic texture) are used. Material parameters correspond to an austenitic stainless steel. The scatter is evaluated using the N90/N10 ratio with N90 (N10) the predicted number of cycles for initiation in 90% (10%) of the specimen. Scatter effects are predicted for small k values (Fig. 2 a) and b), small specimen and large grain sizes). Scatter increases with decreasing applied stress, as is experimentally observed. But, for usual specimen and grain sizes, the predicted scatter is very small when compared with experimental results concerning scatter in the number of cycles to failure. For example, if $k > 400$, the computed torsion scatter becomes negligible (this corresponds to $D = 2\text{mm}$ and $\Phi = 0.1\text{mm}$) (Fig. 3 a) and b)). These Figures are obtained when considering the grain size as constant. They show that there is no specimen size effect for usual specimen and grain sizes. It agrees with experiments which show that a specimen size effect is observed for usual specimen only if loadings leading to a stress gradient through the specimen thickness are applied (bending for example) [5].

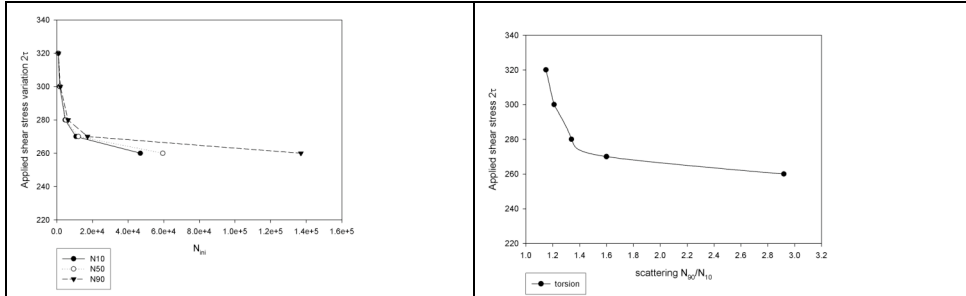


Figure 2: a) simulated Wöhler's curve. Torsion, $k=50$. Probability of 10%, 50% and 90% of crack initiation among specimen; b) Scatter evolution with respect to the applied shear stress (N_{90}/N_{10}). Specimen and material parameters: $k=50$, $\Phi=0.025\text{mm}$, $\tau_0=125\text{MPa}$, $E=200\text{GPa}$, $\nu=0.3$ and $C\tau_s/\Phi p^2(1-\nu)^2=10^6\text{MPa}^2$.

Grain size effect is reproduced. Two grain size effects are in fact taken into account. First, the number of cycles to initiation in a given grain is inversely proportional to its size (eqn (1)). This is due to the slip band geometrical factor which appears when solving the inclusion problem using either Eshelby's solution (bulk slip band) [6] or Finite Element computations (surface slip band) [7]. Second, the statistical computations permit us to take into account the number of surface grains along the gauge length, k . The smaller is the grain size, the larger is the number of surface grains, k . Therefore, the maximal resolved shear stress among the k ones should be higher and the number of cycles to initiation should be smaller. But, for a given grain size, as shown by Fig. 3 a) and b), this effect is saturated when k is higher than 400. In this case, and with an usual specimen size, computations show that the maximal Schmid factor is already reached for larger grain sizes and a decrease of the grain size would not lead to an increase of the maximal Schmid factor and resolved shear stress. Finally, the first grain size effect dominates which gives a number of cycles to crack nucleation inversely proportional to the grain size. This agrees quite well with the experimental results of Nagase et al. [4]. But, it should be noticed that our model predicts the influence of grain size on the numbers of cycle to initiation whereas Nagase et al. experiments permit the authors to evaluate the influence on the number of cycles to failure.

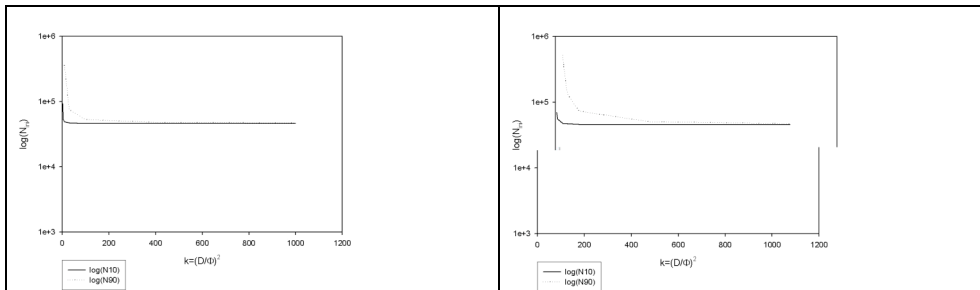


Fig. 3: a) Evolution of the computed numbers of cycles of crack initiation with respect to the specimen size. Tension-compression ; b) Cyclic torsion (Tresca stress amplitude : 260MPa).

4 DISCUSSION

The predicted scatter is smaller than the observed ones. For example, the N90/N10 ratio observed during the experiments detailed in [3,5] is about 10. It can be either due to the crude hypothesis of our model or to a bias in the computation/experiment comparison (predicted scatter concerns crack nucleation whereas experimental scatter concerns both nucleation and propagation phases). Other scatter causes are involved too (defects).

For computing the resolved shear stress and number of cycles to nucleation, a crude hypotheses has been made. The stress tensor was supposed to be homogeneous in the whole polycrystal. Some sources of heterogeneity and dispersion have been neglected such as crystalline cubic elasticity and plasticity. Because of its crystalline structure, the behaviour of each grain is not isotropic. And because of misorientations between neighbour grains, heterogeneities arise. As high-cycle fatigue and small applied stresses are considered, we focus on cubic elasticity. It applies to Face Cubic Centred (FCC) and Body Cubic Centred (BCC) crystals. It is defined by three parameters, C_{11} , C_{12} and C_{44} . An anisotropy factor is classically defined: $a=2 C_{44}/(C_{11}-C_{12})$. It is equal to μ_{\max}/μ_{\min} with μ_{\max} (μ_{\min}) the maximal (minimal) elastic shear modulus obtained when considering all shear systems in a continuous framework. It is equal to 1 for an isotropic material. The anisotropy factor is high for copper ($a=3.3$) and austenite ($a=3.4$). The higher is the anisotropy factor, the more anisotropic is the metal. As the local elastic shear modulus (with respect to the shear system with the maximal macroscopic shear stress) varies strongly depending on the grain crystallographic orientation, large neighbour effects can be suspected. These effects have already been studied by Pommier [10]. But, in her study, neither well-oriented grains nor resolved shear stress were considered even if they are of primary concern in fatigue damage initiation (see observations of [2,9]). To evaluate the neighbour effect involved, finite element computations are carried out (CASTEM2000 software). The mesh is composed of a small aggregate located at the free surface of a large macroscopic matrix. A well-oriented grain is located in the middle of the aggregate (Fig. 4 a)). The crystallographic orientations of the neighbouring grains are chosen randomly whereas the orientation of the well-oriented grain is kept constant. Three computation cases are considered: torsion test (the well-oriented slip system of the grain is of type A [7]) and tensile-compression (either type A or B slip system [7]). For each case, computations are carried out for 40 microstructures. The computation results show that two effects are involved. First, an average effect of the elastic anisotropy induces a decrease of the resolved shear stress in the well-oriented grain when compared to the macroscopic maximal shear stress. It concerns the resolved shear stress averaged on the 40 computations for each loading and type A/B case. The decrease is due to the fact that the well-oriented grain elasticity shear modulus is smaller than the macroscopic one. Second, there is a scatter effect too. It is due to the random neighbour grain orientations.

This more accurate grain shear stress distribution gives more scatter than a simple Schmid factor approach. But, even if this distribution is used for computing the number of cycles to initiation distribution, there are still enough grains with a high resolved shear stress at the surface of usual specimens to induce crack initiation with no delay at about the same numbers of cycles. And the predicted scatter in the number of cycles to initiation is once more negligible for usual specimen and grain sizes. After crack initiation, microstructure barriers such as grain boundaries can slow down more or less the stage I crack propagation. These could explain the scatter in the number of cycles to failure for high-cycle fatigue. Work is in progress for modeling the scatter effect due to the short crack propagation [11].

REFERENCES

- [1] Miller, K. J., Fatigue and Fracture, ASTM STP 1296, p. 267, 1996.
- [2] Villechaise, P., Mineur, M., Mendez, J., Fatigue02, A. Blom ed., EMAS, p. 3221, 2002.
- [3] Bastenaire, P., ASTM STP 511, 1972.
- [4] Nagase, Y., J. Yamamoto, J., and Sawaki, Y., Fatigue 90, H. Kitagawa, T. Tanaka ed., MCEP, p. 67, 1990.
- [5] Brand, A., Flavenot, J. F., Grégoire, R., and Tournier, C., Recueil de données technologiques sur la fatigue, Publications du CETIM, France 1980.
- [6] Kato, M., Onaka, S., Mori, T., and Mura, T., Script. Metall., 18, p. 1323, 1984.
- [7] Sauzay, M., Gilormini, P., Th. Appl. Fract. Mech., 38, p. 53, 2002.
- [8] Mughrabi, H., Wang, R., Differt, K., and Essmann, U., ASTM STP 811, p. 5, 1983.
- [9] Man, J., Obrtlík, K., Polak, J., Acta Materialia, 50, p. 3767, 2002.
- [10] Pommier, S., Fatigue Fract. Engng. Mater. Struct., 25, p. 331, 2002.
- [11] Bertolino, G., Doquet, V., Sauzay, M., Int. J. Fat. , submitted, 2004.